



Short communication

# Electro-oxidation of formic acid on carbon supported Pt-Os catalyst

Wei Liu, Junjie Huang\*

College of Chemistry &amp; Chemical Engineering, Shaoxing University, Shaoxing 312000, PR China

## ARTICLE INFO

## Article history:

Received 17 December 2008

Accepted 17 December 2008

Available online 30 December 2008

## Keywords:

Fuel cell

Formic acid

Pt-Os catalyst

Nano

Electrochemical oxidation

## ABSTRACT

Pt-Os (3:1)/C catalyst was prepared through the route of thermal decomposition of metallic carbonyl cluster. TEM image showed Pt-Os nanoparticles were well dispersed on carbon substrate with an average particle size of  $2.2 \pm 0.9$  nm. XRD pattern indicated Pt-Os has a face-centered cubic crystal structure. Characterized by cyclic voltammetry and chronoamperometry, Pt-Os (3:1)/C catalyst shows a superior electro-catalytic activity to formic acid oxidation in comparison with Pt/C catalyst. This improved electro-catalytic performance was mainly due to the fine dispersion of Pt-Os nano particles and bi-functional effect.

© 2008 Elsevier B.V. All rights reserved.

## 1. Introduction

Formic acid has been widely studied as an alternative to methanol in fuel cell system due to its special characters [1]. Compared with methanol, formic acid is more safety to human, can be used as food additive, which was approved by the US Food and Drug Administration. Formic acid is also a strong electrolyte, which is good to the transportation of electron and proton within the anode compartment. A reductive crossover of formic acid will not only improve the overall cell efficiency, but also allow the use of high feed concentration of formic acid, which will benefit for water management [2].

In fuel cell system, formic acid oxidation takes place through a widely accepted dual path mechanism including direct oxidation mechanism and indirect oxidation mechanism, proposed earlier by Capon and Parsons [3]. In practice, platinum is a widely used electro-catalyst in fuel cells, but its electro-catalytic activity to formic acid oxidation was heavily hindered by  $\text{CO}_{\text{ad}}$  intermediates produced by formic acid indirect oxidation. In order to get rid of  $\text{CO}_{\text{ad}}$  intermediates more efficiently and improve the activity of Pt catalyst greatly, various efforts have been devoted to how to mitigate  $\text{CO}_{\text{ad}}$  intermediates, such as alloying Pt with other metals [4–6] or using other catalyst without metallic Pt (Pd-based catalysts) [7]. Markovic et al. [4] found that Pt-Ru (1:1) had an improved effect to formic acid oxidation in comparison with pure Pt or pure Ru. This improved performance was explained by bi-function mechanism, in which Pt is to absorb and dehydrogenate formic acid molecules,

Ru is to activate water and produce oxygen-containing species at lower potential. This oxygen-containing species have the function to oxidize  $\text{CO}_{\text{ad}}$  intermediates, which can space Pt sites for formic acid molecules' adsorption. For Pt-Bi catalyst, Macia et al. [5] use the theory of an electronic effect to elucidate its improved electro-catalytic activity to formic acid oxidation. In which, Bi can withdraw electron from its nearest neighbor platinum atoms, resulting in a decreasing electron interaction between Pt and  $\text{CO}_{\text{ad}}$  intermediates, so the absorbed CO intermediates can be oxidized more easily.

With the aim to search for an efficient catalyst to formic acid oxidation, Pt-Os (3:1)/C catalyst was prepared through the route of thermal decomposition of PtOs carbonyl cluster, and its electro-catalytic performance to formic acid oxidation was investigated by cyclic voltammetry (CV) and chronoamperometry.

## 2. Experimental

20 wt.% Pt-Os/C catalyst was prepared according to literature [6]. Briefly, Pt and Os carbonyl complexes were synthesized simultaneously using methanol as solvent through the reaction of Pt and Os salts with CO gas at about 55 °C for 24 h with constant mechanical stirring until the solution turned green. Sodium acetate must be added into methanol solution before the reaction, and its amount should be adjusted to the sodium acetate/Pt with molar ratio of 8:1. After the synthesis of Pt-Os carbonyl complexes, Vulcan XC-72 carbon (American Cabot Company) (4 times amount of PtOs in weight) was added to the green solution under  $\text{N}_2$  gas flow and stirred at about 55 °C for more than 6 h. Subsequently, the solvent was removed and the powder was subjected to in situ heat treatment at 185 °C for 5 h under hydrogen. After the thermal treatment, the obtained sample was washed with distilled water until no chlo-

\* Corresponding author. Tel.: +86 575 88341528; fax: +86 575 88341528.  
E-mail address: [hjj@zscas.edu.cn](mailto:hjj@zscas.edu.cn) (J. Huang).

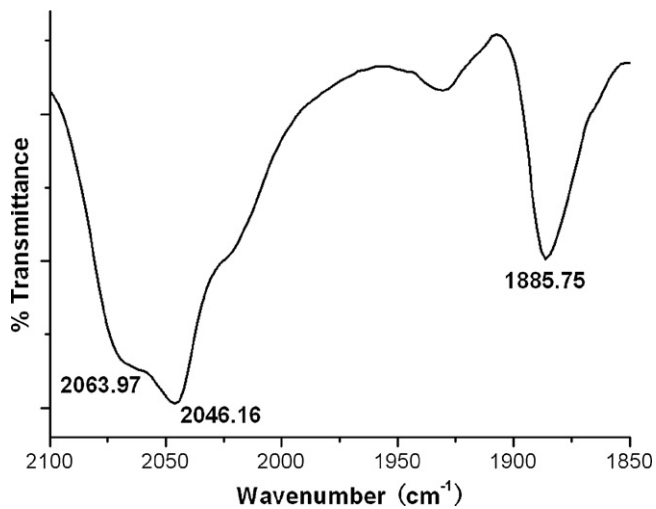


Fig. 1. In situ FTIR spectrum of Pt-Os carbonyl clusters.

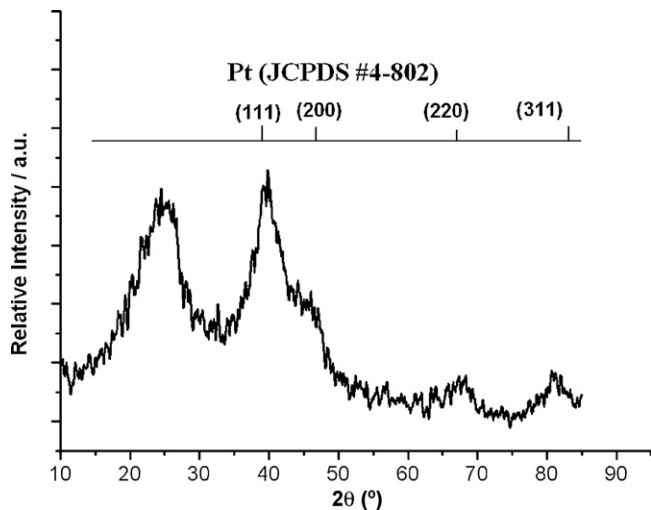
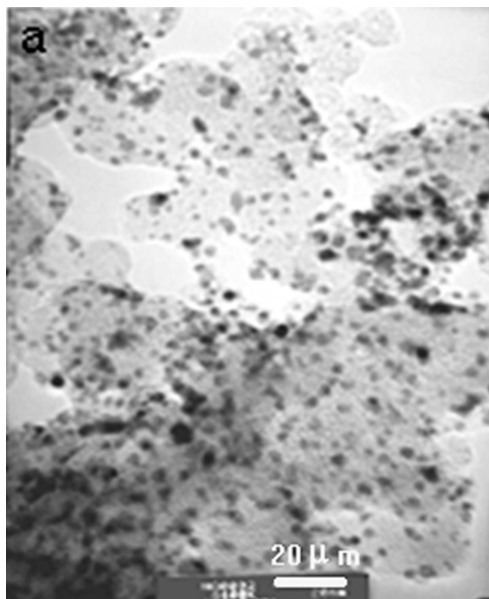


Fig. 2. X-ray diffraction patterns of Pt-Os/C.



rine ions were detected and then dried under vacuum for 12 h at about 50 °C. The composite of Pt to Os measured by ICP is 74.3:25.7 (molar ratio), which is almost the same as the theoretical value of 3:1.

Porous electrodes were prepared as following: 6.6 mg of catalysts, 0.5 mL of Nafion solution (5 wt.%, Aldrich) and 2.5 mL of water were mixed ultrasonically about 10 min. A measured volume (ca. 8  $\mu\text{L}$ ) of this ink was transferred via a syringe onto a freshly polished glassy carbon disk (4 mm in diameter). After the solvents were evaporated at 50 °C under nitrogen, the metal amount loaded on the electrode can be calculated as about 28.0  $\mu\text{g cm}^{-2}$ .

All the potentials are quoted with respect to the reversible hydrogen electrode (RHE) and the electrolyte used was 0.5 M  $\text{HClO}_4$  or 0.5 M  $\text{HCOOH} + 0.5 \text{ M HClO}_4$ . All experiments were performed at a temperature of  $30 \pm 1$  °C.

Powder X-ray diffraction (XRD) measurement of Pt-Os/C was carried out on a Japanese Rigaku D/max-rC X-ray diffractometer using Cu-K radiation. The morphology of Pt-Os/C was characterized by transmission electron microscopy (TEM) using JEM-2010 instrument with a point resolution of 0.14 nm. Elemental analysis of as-prepared catalyst was performed on an inductively coupled plasma (ICP) atomic emission spectrometer (PS-I, Leeman) and elemental analyzer (Leeman). The structure of carbonyl cluster was characterized by Fourier Transform Infrared Spectroscopy (FTIR) (Nexus 670, America Nicolet Company). Surface information of Pt-Os/C catalysts has been characterized by X-ray photoelectron spectroscopy (XPS) on an Escalab Mark II spectrometer (VG Scientific Ltd., England) using Mg K X-ray radiation with a mean energy of 1253.6 eV. CV and chronoamperometry were carried out on a CHI660 electrochemical workstation (CHI Company, USA) in a conventional three-electrode cell; Pt foil and saturated calomel electrode were used as the counter and the reference electrode respectively.

### 3. Results and discussion

Fig. 1 is the in situ FTIR spectrum of Pt-Os carbonyl clusters. Three vibration bands at 2064, 2046 and 1886  $\text{cm}^{-1}$  can be observed obviously, which are related to the characteristic bands of bonded CO group. The first two bands should be assigned to the vibration peaks of linear-CO group in the Pt and Os carbonyl clusters

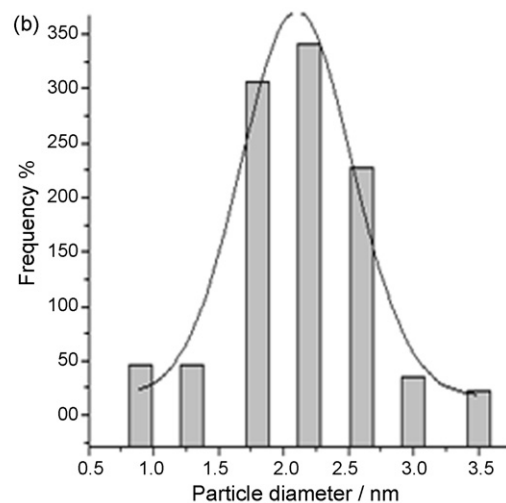


Fig. 3. TEM image of Pt-Os (3:1)/C catalyst (a) with 20% metal loading and its corresponding particle size distribution histogram (b).

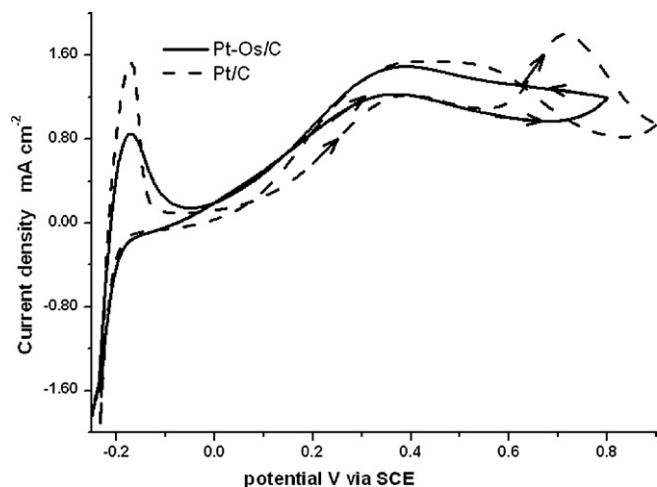


Fig. 4. CVs of methanol oxidation on the (a) Pt-Os (3:1)/C and (b) E-TEK Pt/C catalysts at a scan rate of  $5 \text{ mV s}^{-1}$ . Current densities are normalized to the geometric surface area.

respectively [8,9] and the last one should be related to the vibration peaks of bridge-CO group in Pt carbonyl cluster. As reported in literature [9], Os carbonyl cluster only has linear-CO group, so the vibration band at  $1886 \text{ cm}^{-1}$  should be related to bridge-CO group in Pt carbonyl cluster. Compared with the vibration band ( $2060 \text{ cm}^{-1}$ ) of linear-CO in pure Pt carbonyl cluster [8], the small red shift in the obtained carbonyl cluster indicates that there has an electron interaction between metal Pt and Os. This can be explained as following: because there has an interaction between Pt and Os, Os will withdraw electron from its nearest neighbour Pt, which means the electron donor ability of Pt to CO group will decrease in comparison with that of Pt in pure Pt carbonyl cluster. So, the vibration excited energy of CO group in PtOs carbonyl cluster will be smaller than that in Pure Pt carbonyl cluster, resulting in a red shift of vibration band. The FTIR results also indicate that the Pt and Os carbonyl cluster has been synthesized successfully.

Fig. 2 shows the XRD pattern of Pt-Os (3:1)/C catalyst. With the exception for the first peak of Vulcan XC-72 carbon (located at about  $25^\circ$ ), the other four diffraction peaks can be assigned to four

characteristic peaks of the face-centered cubic (fcc) crystalline Pt according to JCPDS pattern (card 04-802). The diffraction peaks of Pt-Os catalyst are slightly shifted to a higher  $2\theta$  value with respect to the same reflections of bulk Pt, indicative of the alloy formation between Pt and Os. The wide diffraction peaks suggested that the as-prepared Pt-Os alloy existed in a highly disordered form. The lattice parameter ( $a_{\text{fcc}}$ ) of Pt-Os (3:1) alloy catalyst was calculated to be  $3.877 \text{ \AA}$ , which is smaller than that of Pt/C catalyst. The decrease of lattice parameter indicates there has a lattice contraction after alloying. The average size of the Pt-Os (3:1) nanoparticles in the Pt-Os/C catalysts is ca.  $2.2 \text{ nm}$ , which was estimated using Scherrer's equation according to the full width at half maximum of (1 1 1) peak.

Fig. 3 shows the TEM image of Pt-Os (3:1)/C catalyst (a) and its corresponding particle size distribution histogram (b). It can be seen that Pt-Os nanoparticles are well dispersed on the surface of carbon with a relatively narrow particle size distribution. In metallic carbonyl cluster, the Pt and Os atoms are surrounded with bonded CO groups, which can avoid the aggregation of metallic atoms during the thermal treatment process, resulting in small particle sizes. Its' particle size can be measured as about  $2.2 \text{ nm}$  with a standard deviation of  $0.9 \text{ nm}$ , which is similar with the result obtained from XRD.

Fig. 4 presents the CVs of formic acid oxidation on the Pt-Os/C and E-TEK 20% Pt/C electrodes at  $5 \text{ mV s}^{-1}$  in  $0.5 \text{ M HCOOH} + 0.5 \text{ M HClO}_4$  solution. In the CV curve of Pt/C catalyst, two oxidation peaks in the forward located at the potentials of  $0.38$  and  $0.71 \text{ V}$  should be related to the direct oxidation and indirect oxidation of formic acid respectively according to the dual path mechanism [10]. But for Pt-Os/C catalyst, only one oxidation peak in the forward can be observed at the potential of  $0.34 \text{ V}$ , which is related to the direct oxidation of formic acid. Compared with formic acid oxidation on Pt/C catalyst, a small shift of direct oxidation potential (about  $40 \text{ mV}$ ) and the lack of indirect oxidation peak can be found in the CV curve on Pt-Os/C catalyst. Furthermore, the oxidation current at the potential lower than  $0.34 \text{ V}$  on Pt-Os/C is bigger than that on Pt/C. All the results indicated Pt-Os/C catalyst had a good catalytic activity to formic acid oxidation and formic acid oxidation was mainly through the route of direct oxidation path on Pt-Os/C. Such improvement should be explained by bi-function mechanism of Pt and Os, in which Pt was to adsorb and dissociate formic acid molecules and

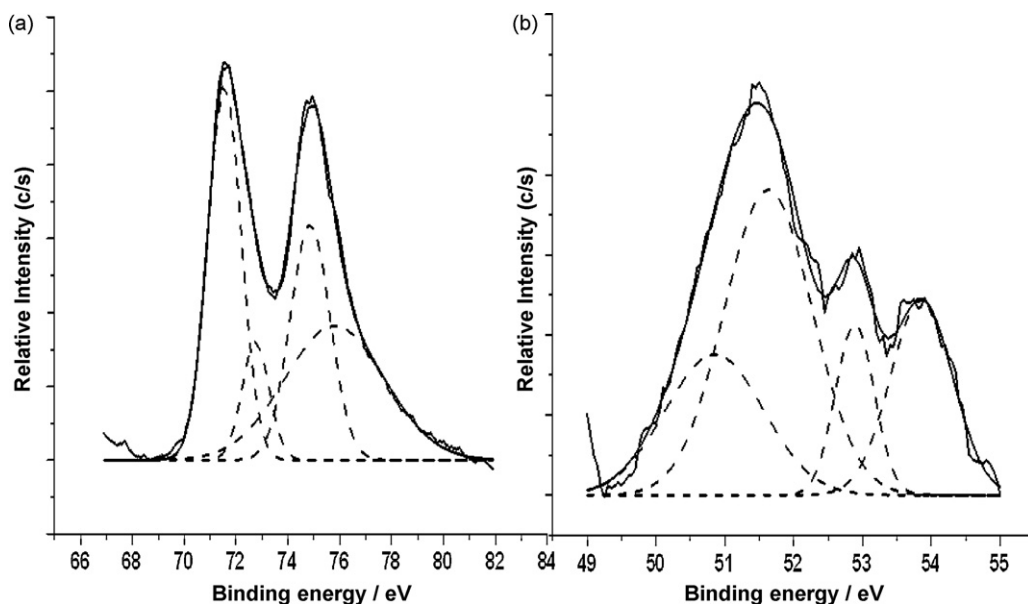
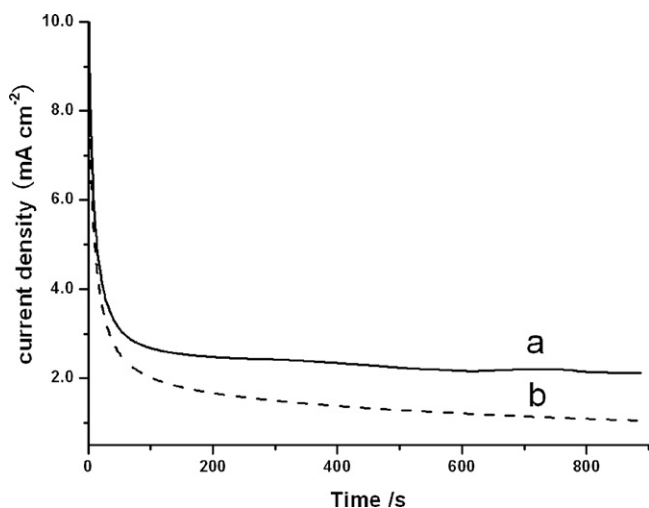


Fig. 5. XPS spectra of the Pt-Os(3:1)/C in the binding energy ranges of Pt 4f (a) and Os 4f (b).



**Fig. 6.** Chronoamperometric curves for oxidation of methanol at 0.36 V/SCE on the (a) Pt-Os (3:1)/C and (b) E-TEK Pt/C catalysts.

the possible role of osmium can supply oxygen-containing species to oxidize the  $\text{CO}_{\text{ad}}$  intermediates at a relative low potential. As reported in literatures [11,12], Os is easy to dehydrogenate water at low potential and produce oxygen-containing species. Another possible explanation should be the electron effect between Pt and Os according to XPS results in the following part, the strong electron withdrawing ability can decrease the interaction between the metallic platinum and intermediates, which make  $\text{CO}_{\text{ad}}$  intermediates oxidize easily.

Fig. 5 shows the XPS results of Pt-Os (3:1)/C sample. The obtained XPS spectra in the binding energy ranges of Pt 4f/Os 4f as well as their Gaussian peaks are shown in Fig. 5a and b respectively. In Fig. 5a, according to the curve fitting result two states of Pt species can be assigned to, the first doublet located at ca. 71.6 eV (Pt  $4f_{7/2}$ ) and 74.8 eV (Pt  $4f_{5/2}$ ) is related to metallic Pt according to literature [13]. But, the Pt  $4f_{7/2}$  binding energy of metallic Pt is slightly higher than the previously reported results for bulk Pt or platinised carbon electrode ( $4f_{7/2} = 71.2$  eV) [14]. Such shift indicates that Os specie has the ability to withdraw the electrons strongly from metallic Pt. the second doublet located at ca. 72.6 eV (Pt  $4f_{7/2}$ ) and 75.8 eV (Pt  $4f_{5/2}$ ) should be related to PtO and/or  $\text{Pt}(\text{OH})_2$  according to literature [12]. In Fig. 5b, two states of Os species can be found in the Pt-Os/C catalyst. The Os 4f signal at about 50.5 eV and 52.9 eV is assigned to metallic osmium [15]. Another doublet located at ca. 51.5 eV and 54.3 eV should be assigned to the Os  $4f_{7/2}$  and  $4f_{5/2}$  of the  $\text{OsO}_2$  species [15]. The obtained metallic Os 4f binding energies are slightly lower than that reported in other literature [15]. Such

shift could be due to the interaction between the Pt and Os, which is in a good agreement with the XPS results of Pt.

Fig. 6 shows the chronoamperometric curves for formic acid oxidation on Pt-Os (3:1)/C and E-TEK 20% Pt/C catalysts. From the data, all catalysts showed some decay in current density, the possible reason should be the poisoning effect by  $\text{CO}_{\text{ad}}$  intermediates. As the polarizing time extending, the catalytic stabilization of Pt-Os (3:1)/C to formic acid oxidation is better than that of E-TEK Pt/C catalyst, which was mainly due to the easier removal of poisonous intermediates on PtOs than pure Pt.

#### 4. Conclusions

The catalytic performance of Pt-Os/C catalyst was investigated by the cyclic voltammograms and the chronoamperometric method. Results show that Pt-Os/C catalyst has a superior electrocatalytic activity to formic acid oxidation in comparison with Pt/C catalyst. This improved behavior to formic acid oxidation should be due to the following reasons: the first is the bi-function mechanism, in which Pt mainly absorb and dehydrogenate formic acid molecular, Os activate water to produce oxygen-containing species at low potential, these oxygen-containing species is easy to oxidize intermediates locating on the Pt sites; the second is the electron effect between metal Pt and Os, the strong electron withdrawing ability of Os leads to the decreased interaction between the Pt and intermediates. The influence of the ratio of Pt to Os will be studied in progress in detail.

#### Acknowledgement

This work was supported by the programme of Shaoxing University (04LG1006).

#### References

- [1] Y. Zhu, S.Y. Ha, R.I. Masel, J. Power Sources 1 (2004) 308.
- [2] C. Rice, S. Ha, R.I. Masel, J. Power Sources 111 (2002) 83.
- [3] A. Capon, R. Parsons, J. Electroanal. Chem. 44 (1973) 1.
- [4] N. Markovic, H. gasteiger, P. Ross Jr., X. Jiang, I. Villegas, Electrochim. Acta 40 (1995) 91.
- [5] M.D. Macia, E. Herrero, J.M. Feliu, J. Electroanal. Chem. 554–555 (2003) 25.
- [6] J. Huang, H. Yang, Q. Huang, J. Electrochem. Soc. 15 (2004) A1810.
- [7] Y. Zhu, Z. Khan, R.I. Masel, J. Power Sources 139 (2005) 15.
- [8] G. Longoni, P. Chini, J. Am. Chem. Soc. 11 (1976) 7225.
- [9] R.B. King, J. Organomet. Chem. 478 (1994) 13.
- [10] X. Wang, J.M. Hu, I.M. Hsing, J. Electroanal. Chem. 562 (2004) 73.
- [11] J. Kua, W.A. Goddard III, J. Am. Chem. Soc. 121 (1999) 10928.
- [12] Y. Zhu, C.R. Cabrera, Electrochem. Solid-State Lett. 4 (2001) A45.
- [13] A.K. Shukla, A.S. Arico, K.M. Khatib, P.L. Antonucci, Appl. Surf. Sci. 137 (1999) 20.
- [14] B.J. Kennedy, A. Hamnett, J. Electroanal. Chem. 283 (1990) 271.
- [15] A. Hamnett, B.J. Kennedy, Electrochim. Acta 33 (1988) 1613.